ACS OMEGA

Article

http://pubs.acs.org/journal/acsodf

New Heteroleptic Cobalt Precursors for Deposition of Cobalt-Based Thin Films

Seong Ho Han,[†,‡] Sheby Mary George,[†] Ga Yeon Lee,[†] Jeong Hwan Han,[†] Bo Keun Park,[†] Chang Gyoun Kim,[†] Seung Uk Son,[‡] Myoung Soo Lah,[§] and Taek-Mo Chung*[,†]

[†]Thin Film Materials Research Center, Korea Research Institute of Chemical Technology, 141 Gajeong-ro, Yuseong-gu, Daejeon 34114, Republic of Korea

[‡]Department of Chemistry and Department of Energy Science, Sungkyunkwan University, 2066 Seobu-ro, Jangan-gu, Suwon-si, Gyeonggi-do 16419, Republic of Korea

[§]Interdisciplinary School of Green Energy, Ulsan National University of Science and Technology, UNIST-gil 50, Ulsan 689-798, Republic of Korea

ABSTRACT: A new series of heteroleptic complexes of cobalt were synthesized using aminoalkoxide and β-diketonate ligands. The complexes, $[Co(dmamp)(acac)]_2$ (**3**), $[Co(dmamp)(tfac)]_2$ (**4**), $[Co(dmamp)(hfac)]_2$ (**5**), $[Co(dmamp)(tmhd)]_2$ (**6**), and $[Co(dmamb)(tmhd)]_2$ (**7**), were prepared by two-step substitution reactions and studied using Fourier transform infrared spectroscopy, mass spectrometry, elemental analysis, and thermogravimetric analysis (TGA). Complexes **3**−**7** displayed dimeric molecular structures for all of the complexes with cobalt metal centers interconnected by μ_2-O bonding by the alkoxy oxygen atom. TGA and a thermal study of the complexes displayed high volatilities and stabilities for complexes **6** and **7**, with sublimation temperatures of 120 °C/0.5 Torr and 130 °C/0.5 Torr, respectively.

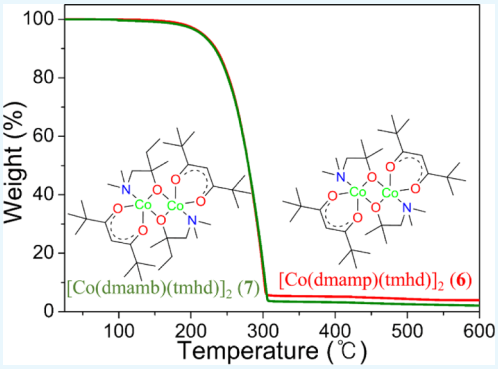

INTRODUCTION

Cobalt is attractive because of its wide variety of applications, such as catalysis,[1] protective coatings,[2] magnetic information storage,[3] and sensor systems.[4] In microelectronics, the applications of cobalt/cobalt-based thin films include their use as the lining material within interconnected trenches,[5] metallic interconnections, ohmic contacts in silicon-based devices,[6] and as Schottky contacts in the field of optoelectronics.[7] Thin films of cobalt and cobalt oxide are also useful as components of energy storage devices, such as $LiCoO_2$ in lithium-ion batteries.[8] In the last decades, cobalt-based thin films have gained a renewed interest in light of the discovery of giant magnetoresistance[9] and tunneling magnetoresistance[10] in multilayer structures for devices using these phenomena.

Many techniques have been used to deposit thin films for these applications. Among them, the most common methods are chemical vapor deposition (CVD) and atomic layer deposition (ALD) because of their potential to produce highly conformal coatings. As electronic devices become smaller and more complex, conformality has become a very important requirement for the deposited thin films. For all of these applications and for the deposition of quality thin films, we require precursors with suitable properties, such as good volatility, thermal stability, and chemical reactivity (leading to pure film deposition). The known precursors of cobalt include dicobalt octacarbonyl,[11] cobalt acetylacetonate,[12] cobalt bis(*N*,*N*′-diisopropylacetamidinate),[13] cobalt bis(*N*,*N*-di-*tert*-butylacetamidinate),[13b] bis(cyclopentadienyl)cobalt,[14] cyclopentadienyl cobalt dicarbonyl,[1c,15] cobalt nitroso tricarbonyl,[16] cobalt hydride tris(trialkylphosphite),[17] bis(*N*-*tert*-butyl-*N*′-ethylpropionamidinato) cobalt(II),[18] bis(1,4-di-*tert*-butyl-1,3-diazadienyl) cobalt,[19] and cyclopentadienyl-cobalt(III)-(diazabutadiene).[20] The observed drawbacks of these precursors include their slow evaporation kinetics, unwanted reactions in the vapor state, film contamination with carbon, low thermal stability, and a high deposition temperature. The design and synthesis of new metal precursors are continuous processes because of the demand for better-performing precursors under a variety of conditions.

Recently, several works, including our own,[21] showed the importance of heteroleptic precursors with improved properties. Most of the common precursors are homoleptic in nature, where the identical ligands are bonded to the metal center. In contrast, a heteroleptic precursor is a metal complex with distinct ligands attached to the metal center. The published results indicate that a heteroleptic precursor designed by a suitable ligand selection could have several better properties than its parent homoleptic precursor. Even though the selection of suitable ligands for heteroleptic metal precursors is as challenging as designing a new ligand for homoleptic

Received: June 16, 2017
Accepted: August 21, 2017
Published: September 6, 2017

DOI: 10.1021/acsomega.7b00800
ACS Omega 2017, 2, 5486−5493

Scheme 1. Synthesis of Complexes 1−7

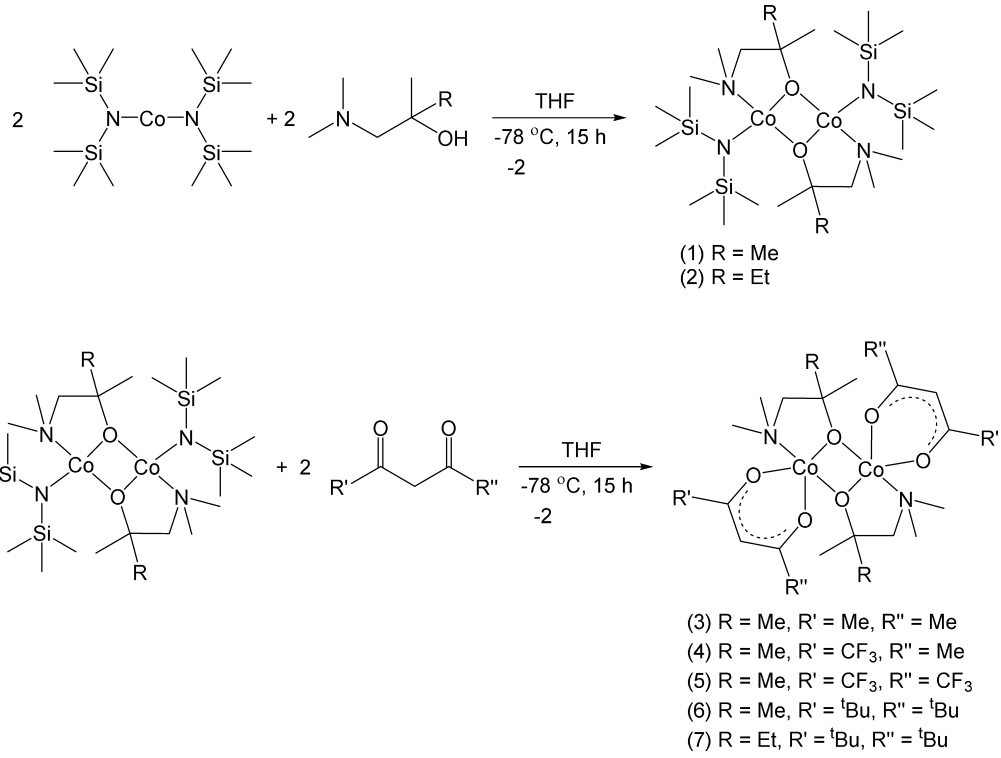

Table 1. Crystallographic Parameters of Complexes 1 and 3−7[a,b]

compound	1	3	4	5	6	7
empirical formula	$C_{24}H_{64}Co_2N_4O_2Si_4$	$C_{22}H_{42}Co_2N_2O_6$	$C_{11}H_{18}CoF_3NO_3$	$C_{22}H_{30}Co_2F_{12}N_2O_6$	$C_{34}H_{66}Co_2N_2O_6$	$C_{36}H_{70}N_2O_6Co_2$
formula weight	671.01	548.43	328.19	764.34	716.75	744.80
T/K	100(2)	100(2)	100(2)	100(2)	100(2)	173(2)
crystal system	monoclinic	orthorhombic	orthorhombic	orthorhombic	triclinic	triclinic
space group	$P2(1)/n$	$Pbca$	$Pbca$	$Pbca$	$P\bar{1}$	$P\bar{1}$
a (Å)	9.2665(2)	12.5460(3)	12.8499(5)	12.9686(2)	9.3999(2)	10.095(2)
b (Å)	20.0041(5)	9.9766(2)	10.0409(4)	10.2305(2)	10.2161(2)	10.147(2)
c (Å)	9.7333(2)	20.9672(5)	21.5189(9)	21.9931(4)	11.5967(2)	11.580(2)
α (deg)	90	90	90	2917.94(9)	85.0140(10)	82.58(3)
β (deg)	95.5500(10)	90	90	90	83.1030(10)	83.11(3)
γ (deg)	90	90	90	90	62.6430(10)	63.63(3)
V (Å ^{3})	1795.78(7)	2624.39(10)	2776.47(19)	90	981.29(3)	1051.2(4)
Z	2	4	8	4	1	1
density (g/cm^{-3})	1.241	1.388	1.570	1.740	1.213	1.176
absorption coefficient	1.082	1.301	1.273	1.253	0.885	0.829
F(000)	724	1160	1352	1544	386	402
crystal size (mm^3)	0.24 × 0.18 × 0.10	0.28 × 0.18 × 0.02	0.20 × 0.20 × 0.03	0.16 × 0.12 × 0.05	0.16 × 0.10 × 0.06	0.16 × 0.15 × 0.12
θ range for data collection (deg)	2.036−28.437	1.943−28.369	1.893−28.269	1.852−28.318	1.770−28.474	3.185−27.484
index ranges	$-12 \le h \le 12$, $0 \le k \le 26$, $0 \le l \le 13$	$0 \le h \le 16$, $0 \le k \le 13$, $-28 \le l \le 0$	$0 \le h \le 17$, $0 \le k \le 13$, $-28 \le l \le 0$	$0 \le h \le 17$, $0 \le k \le 13$, $-29 \le l \le 0$	$-12 \le h \le 12$, $-13 \le k \le 13$, $0 \le l \le 15$	$-13 \le h \le 12$, $-12 \le k \le 13$, $-14 \le l \le 14$
reflections collected	4512	3285	3434	3631	4912	9870
independent reflections	4512 [R(int) = 0.0000]	3285 [R(int) = 0.0000]	3434 [R(int) = 0.0000]	3631 [R(int) = 0.0000]	4912 [R(int) = 0.0000]	4732 [R(int) = 0.0408]
goodness-of-fit on F^2	1.049	1.069	1.084	1.027	1.027	1.046
final R indices [$I > 2\sigma(I)$]	$R1$ = 0.0292, $wR2$ = 0.0761	$R1$ = 0.0283, $wR2$ = 0.0649	$R1$ = 0.0723, $wR2$ = 0.2129	$R1$ = 0.0355, $wR2$ = 0.0802	$R1$ = 0.0334, $wR2$ = 0.0715	$R1$ = 0.0556, $wR2$ = 0.1098
R indices (all data)	$R1$ = 0.0338, $wR2$ = 0.0794	$R1$ = 0.0381, $wR2$ = 0.0695	$R1$ = 0.0966, $wR2$ = 0.2304	$R1$ = 0.0471, $wR2$ = 0.0876	$R1$ = 0.0449, $wR2$ = 0.0763	$R1$ = 0.0829, $wR2$ = 0.1194

[a] $R1 = (\sum||F_o| - |F_c||)/\sum|F_o|$. [b] $wR2 = [\sum\omega(F_o^2 - F_c^2)^2/\sum\omega(F_o^2)^2]^{1/2}$.

DOI: 10.1021/acsomega.7b00800
ACS Omega 2017, 2, 5486−5493

precursors, the heteroleptic precursors are advantageous because of the availability of several ligands and their complexes with known properties to choose from.

Here, we demonstrate the synthesis and characterization of new heteroleptic cobalt precursors with a combination of aminoalkoxide (1-dimethylamino-2-methyl-2-propoxide (dmamp) and 1-dimethylamino-2-methyl-2-butoxide (dmamb)) and β-diketonate (2,2,6,6-tetramethylheptan-3,5-dionate (tmhd), acetylacetonate (acac), 1,1,1-trifluoro-2,4-pentanedionate (tfac), and 1,1,1,5,5,5-hexafluoro-2,4-pentanedionate (hfac)) ligands. The complexes, $[Co(dmamp)(acac)]_2$ (**3**), $[Co(dmamp)(tfac)]_2$ (**4**), $[Co(dmamp)(hfac)]_2$ (**5**), $[Co(dmamp)(tmhd)]_2$ (**6**), and $[Co(dmamb)(tmhd)]_2$ (**7**), were prepared by simple substitution reactions using the corresponding ligands and cobalt(II) bis(bis(trimethylsilyl)-amide) $[Co(btsa)_2]$. All of the complexes were characterized using Fourier transform infrared (FT-IR), elemental analysis, thermogravimetric analysis (TGA), and X-ray crystallography. The results demonstrate excellent thermal stabilities and volatilities of these complexes, especially **6** and **7**, which displayed high volatilities and stabilities.

RESULTS AND DISCUSSION

New heteroleptic cobalt complexes were prepared by controlled substitution reactions, as illustrated in Scheme 1. First, the tetrahydrofuran (THF) solution containing $Co(btsa)_2$ was treated with an equivalent amount of an aminoalcohol (dmampH or dmambH) at low temperature. The products, $[Co(dmamp)(btsa)]_2$ (**1**) and $[Co(dmamb)(btsa)]_2$ (**2**), were isolated by extracting with toluene. In the second step, **1** reacted with β-diketones, such as acacH, tfacH, hfacH, and tmhdH, and **2** reacted with tmhdH in THF solutions at low temperature. The products, $[Co(dmamp)(acac)]_2$ (**3**), $[Co(dmamp)(tfac)]_2$ (**4**), $[Co(dmamp)(hfac)]_2$ (**5**), $[Co(dmamp)(tmhd)]_2$ (**6**), and $[Co(dmamb)(tmhd)]_2$ (**7**), were isolated by extracting with hexane. All of the complexes prepared in this work are highly soluble in common organic solvents, such as toluene, hexane, THF, and ether. Additionally, they are quite stable under inert conditions, such as a nitrogen atmosphere.

X-ray-quality crystals of the complexes were obtained from saturated toluene (**1**) and hexane (**3**–**7**) solutions at −30 °C. The crystals of complex **7** exhibited thermal disorder in the β-diketonate (in **7**) chain. Complex **1** crystallized in a monoclinic space group, complexes **6** and **7** crystallized in triclinic space groups, and complexes **3**–**5** crystalized in orthorhombic space groups (Table 1). All of the complexes formed dimers with alkoxy oxygens bridging the two metal centers in the complexes by μ_2–O bonding. This is similar to the results for previously reported group 2 metal complexes $[M(aminoalkoxide)(btsa)]_2$ (M = Mg, Sr, and Ca) and $[M(aminoalkoxide)(tmhd)]_2$ (M = Mg, Sr, Ca, and Ba).[21d,e] In complex **1**, each of the cobalt metal ions was bonded to one btsa ligand and one dmamp ligand, exhibiting a tetrahedral geometry (Figure 1). The bond length between cobalt and nitrogen of the btsa group is recorded as Co–N = 1.9514(13) Å in **1** (Table 2), which is slightly shorter than that previously reported for $[Co\{(N^tBu)_3SMe\}_2]$ (1.9873 (11) Å and 1.9939(10) Å).[22] Similarly, the Co–N bond between cobalt and the dmamp nitrogen atom displayed a bond length of 2.1598(14) Å, which is also shorter than the known Co–N bond lengths in $[Co(acac)_2(TMEDA)]$ and $[Co(acac)_2(DMAPH)]_2$[23] (2.227(5) Å and 2.252(2) Å, respectively). The reaction of β-diketone with **1** and **2** substituted the remaining btsa ligand to afford complexes **3**–**7**. The crystal structures of **3**–**6** displayed penta-coordinated metal centers and trigonal bipyramidal structures. In complexes **3**–**7**, as shown in Figures 2–6, the Co–O bond lengths between the central cobalt ion and the oxygen of the β-diketonate ligands were 2.0017(12), 2.015(3), 2.0187(15), 2.0048(11), and 1.996(7) Å, respectively, which were again shorter than that for similar β-diketonate complexes of cobalt (2.064(4) Å for $[Co(acac)_2(TMEDA)]$, 2.046(3) Å for $[Co(acac)_2(DMAPH)]_2$,[23] 2.034(3) Å for $[Co(acac)_2(py)_2]$, and 2.036(12) Å for $[Co(tmhd)_2(py)_2]$).[24] However, the Co–O bond lengths for complexes **3**–**7** are longer than those in the $Co(thd)_3$ complex (1.869(2) Å)[25] and in $[Co(^tBuNNCHCRO)_2$ (R = ^{t}Bu, ^{i}Pr, Me)][26] (average Co–O bond length is 1.915(1) Å). An increase in the Co1–O1–Co1^i bond angle and relative increase in the Co···Co distances were observed between complex **1** and complexes **3**–**7** (Table 2). This is because the structure changes from a very strained tetrahedral geometry for **1** to a more relaxed and stable trigonal bipyramidal geometry for **3**–**7** by the substitution of the monodentate btsa with bidentate tmhd ligands.

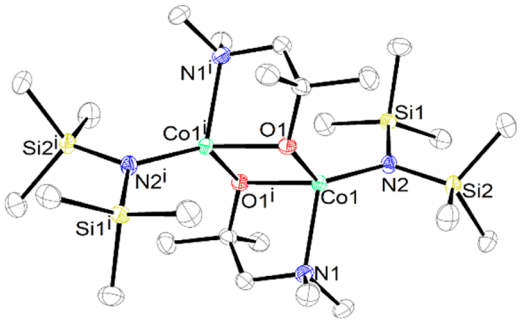

Figure 1. Crystal structure of $[Co(dmamp)(btsa)]_2$ (**1**).

The FT-IR spectra of the compounds confirmed the complex formation. Strong peaks are observed at ν = 2950 cm^{-1} (**1**) and 2963 cm^{-1} (**2**) (Si–CH_3 stretching vibrations) and at 1242 cm^{-1} (**1** and **2**) (Si–CH_3 rocking vibration), confirming the presence of one btsa group in the compounds. The reaction of **1** or **2** with the β-diketones removed the btsa groups and formed **3**–**7**. The FT-IR spectra of complexes **3**–**7** displayed strong peaks at ν = 1601, 1627, 1645, 1583, and 1584 cm^{-1}, respectively, corresponding to the C=O stretching in coordinated β-diketones. The absence of btsa peaks confirmed the complete substitution of the btsa groups by β-diketonate ligands. This is also confirmed by the Co–O stretching observed at ν = 452, 455, 458, 474, and 476 cm^{-1} for complexes **3**–**7**, respectively.[27] The absence of –OH stretching peaks in the FT-IR spectra indicates that the complexes are free of any non-coordinated ligands. The elemental analysis results for the complexes were comparable to the calculated values, considering their sensitivity toward air and moisture.

The mass spectra of the complexes **1**–**7** displayed peaks at m/z = 554, 568, 432, 540, 648, 600, and 614, respectively, which correspond to $[\{M(aminoalkoxide)(\beta\text{-diketonate})\}2(aminoalkoxide)]^+$. These results confirmed that the complexes formed into dimer structures and one aminoalkoxide ligand was easily separated from the complexes due to their high air and moisture sensitivity during mass analyses.

TGA was performed for complexes **3**–**7** from room temperature to 800 °C (Figure 6). Samples for the analysis were prepared inside an argon-filled glovebox, and data

DOI: 10.1021/acsomega.7b00800
ACS Omega 2017, 2, 5486–5493

Table 2. Selected Bond Lengths (Å) and Bond Angles (deg) for Complexes 1 and 3−7

[Co(dmamp)(btsa)]$_2$ (**1**)		[Co(dmamp)(acac)]$_2$ (**3**)		[Co(dmamp)(tfac)]$_2$ (**4**)	
Bond Lengths (Å)					
Co1−N1	2.1598(14)	Co1−O1	1.9453(11)	Co1−O1	1.935(3)
Co1−O1	2.0058(11)	Co1−O2	1.9973(12)	Co1−O2	2.010(3)
Co1−O1^i	2.0149(12)	Co1−O3	2.0061(12)	Co1−O3	2.020(3)
Co1−N2	1.9514(13)	Co1−O1^i	2.0306(11)	Co1−O1^i	2.020(3)
		Co1−N1	2.2646(16)	Co1−N1	2.260(4)
Co1···Co1^i	2.9088(4)	Co1···Co1^i	3.0871(4)	Co1···Co1^i	3.0627(9)
Bond Angles (deg)					
O1−Co1−N1	102.90(5)	O1−Co1−O1^i	78.15(5)	O1−Co1−O1^i	78.54(14)
N1−Co1−O1^i	84.65(5)	O1−Co1−O2	136.84(5)	O1−Co1−O2	136.83(15)
O1−Co1−O1^i	87.32(5)	O1−Co1−O3	129.65(5)	O1−Co1−O3	130.42(15)
N1−Co1−N2	115.49(6)	O1−Co1−N1	80.34(5)	O1−Co1−N1	81.06(14)
O1−Co1−N2	126.35(5)	O1^i−Co1−O2	100.80(5)	O1^i−Co1−O2	100.79(14)
O1^i−Co1−N2	130.32(5)	O1^i−Co1−O3	103.25(5)	O1^i−Co1−O3	102.64(14)
Co1−O1−Co1^i	92.68(5)	O1^i−Co1−N1	158.33(5)	O1^i−Co1−N1	159.54(13)
		O2−Co1−O3	92.98(5)	O2−Co1−O3	92.25(14)
		O2−Co1−N1	93.12(5)	O2−Co1−N1	92.97(14)
		O3−Co1−N1	92.42(5)	O3−Co1−N1	91.76(14)
		Co1−O1−Co1^i	101.85(5)	Co1−O1−Co1^i	101.46(14)
[Co(dmamp)(hfac)]$_2$ (**5**)		[Co(dmamp)(tmhd)]$_2$ (**6**)		[Co(dmamb)(tmhd)]$_2$ (**7**)	
Bond Lengths (Å)					
Co1−O1	1.9342(14)	Co1−O1	2.0995(11)	Co1−O1	1.970(2)
Co1−O2	2.0101(15)	Co1−O2	2.0046(11)	Co1−O2	1.978(2)
Co1−O3	2.0272(14)	Co1−O3	2.0050(12)	Co1−O3	2.015(2)
Co1−O1^i	2.0274(15)	Co1−O1^i	1.9611(11)	Co1−O1^i	1.979(2)
Co1−N1	2.2380(18)	Co1−N1	2.1470(14)	Co1−N1	2.209(3)
Co1···Co1^i	3.0431(5)	Co1···Co1^i	3.0718(4)	Co1···Co1^i	3.064(1)
Bond Angles (deg)					
O1−Co1−O1^i	79.03(6)	O1−Co1−O1^i	81.74(5)	O1−Co1−O1^i	78.23(9)
O1−Co1−O2	132.05(6)	O1−Co1−O2	89.44(5)	O1−Co1−O2	115.98(9)
O1−Co1−O3	136.88(7)	O1−Co1−O3	169.02(5)	O1−Co1−O3	151.18(9)
O1−Co1−N1	81.61(6)	O1−Co1−N1	80.55(5)	O1−Co1−N1	77.51(9)
O1^i−Co1−O2	101.78(6)	O1^i−Co1−O2	121.48(5)	O1^i−Co1−O2	114.43(9)
O1^i−Co1−O3	100.37(6)	O1^i−Co1−O3	108.08(5)	O1^i−Co1−O3	101.46(9)
O1^i−Co1−N1	160.62(6)	O1^i−Co1−N1	104.34(5)	O1^i−Co1−N1	147.81(9)
O2−Co1−O3	90.66(6)	O2−Co1−O3	89.41(5)	O2−Co1−O3	90.68(8)
O2−Co1−N1	91.80(6)	O2−Co1−N1	131.11(5)	O2−Co1−N1	95.17(10)
O3−Co1−N1	93.14(7)	O3−Co1−N1	92.03(5)	O3−Co1−N1	90.00(9)
Co1−O1−Co1^i	100.97(6)	Co1−O1−Co1^i	98.26(5)	Co1−O1−Co1^i	101.77(9)

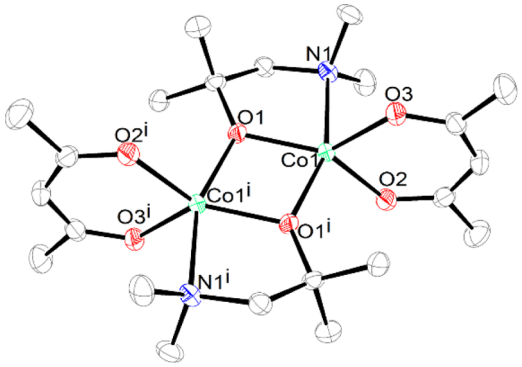

Figure 2. Crystal structure of [Co(dmamp)(acac)]$_2$ (**3**).

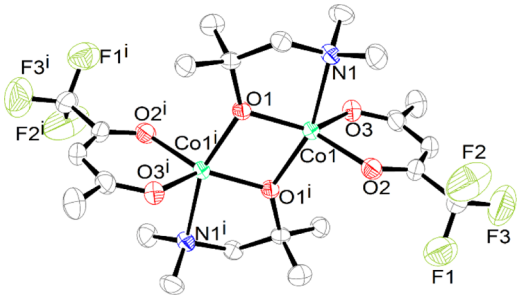

Figure 3. Crystal structure of [Co(dmamp)(tfac)]$_2$ (**4**).

collection was performed under a constant flow of nitrogen to minimize any air contact. The TGA plots of complexes **3**, **4**, and **5** show sharp weight losses of 75, 85, and 90% from 110 to 260 °C (for **3**), 110 to 250 °C (for **4**), and 110 to 220 °C (for **5**), respectively. This indicates the possible vaporization of part of the complex in those temperatures. Further mass losses of 13, 6, and 9% and the final residues of 12, 4, and 6% were observed for **3**, **4**, and **5**, respectively. The second step of the mass loss in the TGA may be the evaporation of some of the fragments resulting from the complex decomposition. In contrast, complexes **6** and **7** displayed clean, single-step TGA curves from 175 to 310 °C with mass losses of 94 and 96%,

DOI: 10.1021/acsomega.7b00800
ACS Omega 2017, 2, 5486−5493

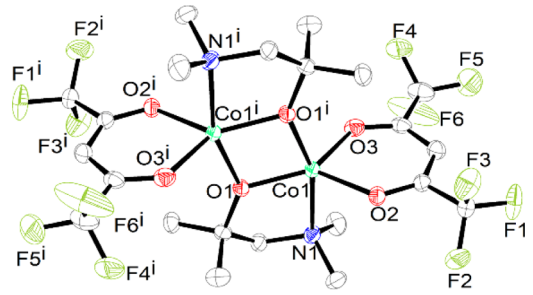

Figure 4. Crystal structure of $[Co(dmamp)(hfac)]_2$ (**5**).

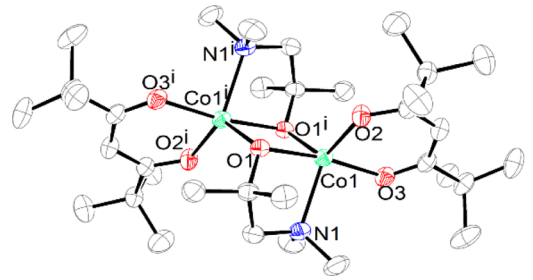

Figure 5. Crystal structure of $[Co(dmamp)(tmhd)]_2$ (**6**).

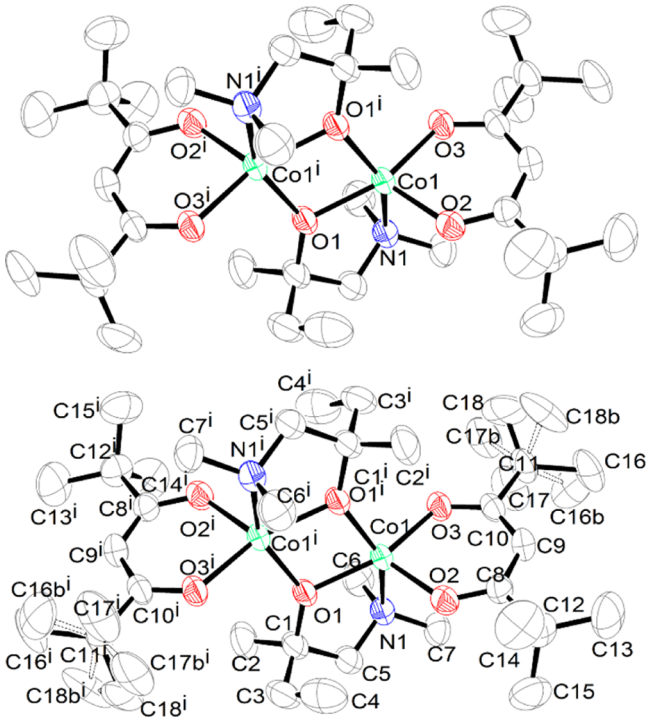

Figure 6. Crystal structure of $[Co(dmamb)(tmhd)]_2$ (**7**).

respectively. The presence of the second step of mass losses for complexes **3**–**5** indicates a possible fragmentation of the samples, whereas complexes **6** and **7** display excellent vaporization and thermal characteristics (Figure 7).

The complexes were subjected to sublimation experiments under a reduced pressure (0.5 Torr) to better understand their volatile characteristics. All of the complexes, except **6** and **7**, remained nonvolatile under those conditions (up to 150 °C/0.5 Torr). Complexes **6** and **7** sublimed at 120 and 130 °C, respectively, with good yields. The sublimed parts of the complexes were further characterized by FT-IR, elemental

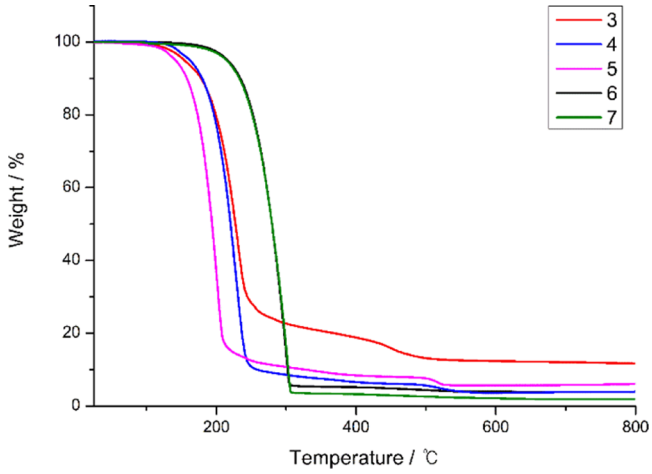

Figure 7. TGA plot of complexes **3**–**7**. Red (**3**), blue (**4**), pink (**5**), black (**6**), and green (**7**).

analysis, and mass spectroscopy to confirm that there were no changes in the structural features and that no decomposition occurred during the process. Complexes **3**–**5** remained nonvolatile in this process and underwent partial decomposition during prolonged heating at elevated temperatures for long period.

Our study reveals the possibility of developing heteroleptic precursors by selecting suitable ligands from a large pool of known ligands. This work reaffirms the importance of heteroleptic complexes as metal precursors because the proper combination of ligands yields better properties than those of their parent homoleptic complexes. In particular, complexes **6** ($[Co(dmamp)(tmhd)]_2$) and **7** ($[Co(dmamb)(tmhd)]_2$) displayed good characteristics with the melting points of 131 and 113 °C, respectively, and the sublimation temperatures of 120 °C/0.5 Torr and 130 °C/0.5 Torr, respectively. These melting temperatures are lower than those of commercial tmhd precursors of cobalt, such as $Co(tmhd)_2$ (143 °C) and $Co(tmhd)_3$ (254 °C). This study clearly demonstrates that well-designed heteroleptic metal precursors can be useful alternatives to overcome the shortcomings of their parent complexes.

CONCLUSIONS

In summary, new heteroleptic complexes of cobalt using aminoalkoxides and β-diketonates were successfully synthesized using controlled two-step substitution reactions with $Co(btsa)_2$. Both the partially substituted first-step compounds and final compounds were obtained as dimers in their crystal structures. The alkoxy oxygen of the aminoalkoxide used in this work acted as a bridge between two cobalt metal centers by μ_2–O bonding. In those complexes, the metal center appeared to have a tetrahedral geometry in **1**, whereas their geometry appeared to be trigonal bipyramidal in complexes **3**–**7**. The TGA curves for complexes **4**–**7** displayed minimal nonvolatile residues, indicating their possible vaporization in the process. The sublimation studies revealed the excellent volatile character of complexes **6** and **7** at 120 and 130 °C under 0.5 Torr, respectively. Even though complexes **3**–**7** were in the dimeric state, all of the complexes displayed good stabilities at high temperatures. In particular, **6** and **7** displayed excellent volatilities and stabilities compared with their respective parent homoleptic complexes available from commercial sources.

DOI: 10.1021/acsomega.7b00800
ACS Omega 2017, 2, 5486–5493

Studies for the application of **6** and **7** as precursors for the deposition of cobalt and cobalt oxide thin films by an ALD process are in progress.

EXPERIMENTAL SECTION

Materials. FT-IR spectra were obtained using a Nicolet Nexus FT-IR spectrophotometer with a 4 mm KBr window or KBr pellets. The KBr pellets for the samples were prepared by a standard pellet technique inside an argon-filled glovebox. The elemental analyses were performed with a Thermo Scientific OEA Flash 2000 analyzer. The thermogravimetric analyses were conducted on a Thermo plus EVO II TG8120 series thermogravimetry and differential thermal analysis instrument under a constant flow of nitrogen. The mass spectra were recorded using a JEOL JMS-700 spectrometer operating in electron ionization (EI) mode. All of the reactions, except for the ligand preparations, were performed under inert and dry conditions using standard Schlenk techniques or in an argon-filled glovebox. $Co(btsa)_2$,[28,29] dmampH, and dmambH were synthesized by a slightly modified literature method.[30] Hexane, THF, and toluene were purified using an Innovative Technology PS-MD-4 solvent purification system. All of the chemicals were purchased from Aldrich and used as received.

General Procedure for the Synthesis of [Co(aminoalkoxide)(btsa)]$_2$ Complexes. A THF solution (10 mL) of aminoalcohol was added dropwise to a solution of $Co(btsa)_2$ in THF (50 mL) at −78 °C with constant stirring and was stirred for 1 h at that temperature. The reaction mixture was slowly warmed to room temperature and then stirred for another 15 h. After the completion of the reaction, the volatiles were removed in vacuo and the residue was extracted into toluene and filtered. The toluene was removed to obtain the crude product. X-ray-quality crystals were grown from a saturated solution in toluene upon cooling at −30 °C.

*[Co(dmamp)(btsa)]$_2$ (**1**).* $Co(btsa)_2$ (2.53 g, 6.96 mmol) and dmampH (0.81 g, 6.96 mmol) were used. Dark blue crystals were obtained. Yield: 2.24 g (90%), mp 90 °C. FT-IR (KBr, cm^{-1}): 2950(s), 1472(m), 1456(m), 1256(s), 1242(s), 1191(w), 1157(m), 1123(w), 1010(w), 981(m), 951(s), 912(m), 877(s), 844(s), 821(s), 788(m), 667(m), 552(w), 484(w). Anal. Calcd for $C_{24}H_{64}N_4O_2Si_4Co_2$: C, 43.0; H, 9.61; N, 8.35. Found: C, 42.3; H, 9.58; N, 7.94. EI-MS: *m/z* calcd for $[Co(dmamp)(btsa)]_2$: 670.28 $[M]^+$; found 554 $[\{Co(dmamp)(btsa)\}_2\text{-}\{dmamp\}]^+$, 175 $[Co(dmamp)]^+$.

*[Co(dmamb)(btsa)]$_2$ (**2**).* $Co(btsa)_2$ (3.79 g, 10 mmol) and dmambH (1.31 g, 10 mmol) were used. Dark green crystals were obtained. Yield: 2.24 g (90%), mp 110 °C. FT-IR (KBr, cm^{-1}): 2963(s), 1465(m), 1383(w), 1242(s), 1181(w), 1131(m), 999(s), 984(s), 965(s), 917(w), 874(s), 838(s), 664(m), 620(w), 597(w), 518(w), 473(w). Anal. Calcd (%) for $C_{26}H_{68}N_4O_2Si_4Co_2$: C, 44.7; H, 9.81; N, 8.01. Found: C, 44.5; H, 9.98; N, 8.00. EI-MS: *m/z* calcd for $[Co(dmamb)(btsa)]_2$: 698.31 $[M]^+$; found 568 $[\{Co(dmamp)(btsa)\}_2\text{-}\{dmamb\}]^+$.

General Procedure for the Synthesis of [Co(aminoalkoxide)(β-diketonate)]$_2$ Complexes. A THF solution (10 mL) of β-diketone was added dropwise to a solution of $[Co(aminoalkoxide)(btsa)]_2$ in THF (50 mL) at −78 °C with constant stirring. The reaction mixture was stirred for 1 h at that temperature and then slowly warmed to room temperature. The reaction mixture was then stirred for another 15 h. After completion of the reaction, the volatiles were removed in vacuo, and the residue was extracted into hexane and filtered. The hexane was then removed to obtain the crude product. X-ray-quality crystals were grown from a saturated solution in hexane upon cooling at −30 °C.

*[Co(dmamp)(acac)]$_2$ (**3**).* $[Co(dmamp)(btsa)]_2$ (**1**) (1.34 g, 2 mmol) and acacH (0.40 g, 4 mmol) were used. The crude product was recrystallized to obtain the pure product of dark green crystals. Yield: 0.54 g (50 %), mp 154 °C. FT-IR (KBr, cm^{-1}): 2968(s), 2917(s), 2856(m), 1601(s), 1516(s), 1459(m), 1413(m), 1396(s), 1352(m), 1299(w), 1259(m), 1210(m), 1194(m), 1153(m), 1128(w), 1033(m), 1019(m), 984(m), 946(m), 921(m), 906(w), 843(w), 796(m), 763(m), 640(m), 567(w), 526(w), 452(w), 430(w). Anal. Calcd for $C_{22}H_{42}N_2O_6Co_2$: C, 48.2; H, 7.72; N, 5.1. Found: C, 48.5; H, 7.77; N, 5.23. EI-MS: *m/z* calcd for $[Co(dmamp)(acac)]_2$: 548.17 $[M]^+$; found 432 $[\{Co(dmamp)(acac)\}_2\text{-}\{dmamp\}]^+$, 257 $[Co(acac)_2]^+$, 158 $[Co(acac)]^+$.

*[Co(dmamp)(tfac)]$_2$ (**4**).* $[Co(dmamp)(btsa)]_2$ (**1**) (1.34 g, 2 mmol) and tfacH (0.62 g, 4 mmol) were used. The crude product was recrystallized to obtain the pure product of dark green crystals. Yield: 0.91 g (69 %), mp 143 °C. FT-IR (KBr, cm^{-1}): 2970(m), 2862(m), 2837(m), 1627(s), 1524(m), 1475(m), 1405(w), 1358(m), 1292(s), 1227(m), 1184(m), 1135(s), 1016(m), 983(m), 943(m), 908(m), 858(m), 842(w), 797(m), 778(m), 729(m), 641(m), 575(m), 528(w), 455(w). Anal. Calcd for $C_{22}H_{46}N_2O_6F_6Co_2$: C, 40.3; H, 5.53; N, 4.27. Found: C, 40.3; H, 5.31; N, 3.86. EI-MS: *m/z* calcd for $[Co(dmamp)(tfac)]_2$: 656.11 $[M]^+$; found 540 $[\{Co(dmamp)(tfac)\}_2\text{-}\{dmamp\}]^+$, 365 $[Co(tfac)_2]^+$, 212 $[Co(tfac)]^+$.

*[Co(dmamp)(hfac)]$_2$ (**5**).* $[Co(dmamp)(btsa)]_2$ (**1**) (1.34 g, 2 mmol) and hfacH (0.83 g, 4 mmol) were used. The crude product was recrystallized to obtain the pure product of dark yellow crystals. Yield: 1.07 g (70 %), mp 120 °C. FT-IR (KBr, cm^{-1}): 2974(m), 1645(s), 1554(m), 1527(m), 1499(m), 1254(s), 1199(s), 1146(s), 1024(w), 981(w), 942(w), 910(w), 798(m), 669(m), 641(w), 586(m), 527(w). Anal. Calcd for $C_{22}H_{30}N_2O_6F_{12}Co_2$: C, 34.6; H, 3.96; N, 3.67. Found: C, 35.3; H, 4.15; N, 3.50. EI-MS: *m/z* calcd for $[Co(dmamp)(hfac)]_2$: 764.06 $[M]^+$; found 648 $[\{Co(dmamp)(hfac)\}_2\text{-}\{dmamp\}]^+$, 473 $[Co(hfac)_2]^+$, 266 $[Co(hfac)]^+$.

*[Co(dmamp)(tmhd)]$_2$ (**6**).* $[Co(dmamp)(btsa)]_2$ (**1**) (1.34 g, 2 mmol) and tmhdH (0.74 g, 4 mmol) were used. The crude product was purified by sublimation (120 °C/0.5 Torr) to obtain a pure solid green product. Yield: 0.90 g (63 %), mp 131 °C. FT-IR (KBr, cm^{-1}): 2963(s), 2861(s), 2829(m), 1583(s), 1569(s), 1546(s), 1531(s), 1503(s), 1454(s), 1412(s), 1398(s), 1354(s), 1246(w), 1225(m), 1207(m), 1185(m), 1153(m), 1135(m), 1020(m), 987(m), 949(m), 906(w), 869(m), 840(w), 797(m), 788(m), 760(w), 738(w), 637(m), 525(w), 474(m), 410(w). Anal. Calcd for $C_{34}H_{66}N_2O_6Co_2$: C, 57.0; H, 9.28; N, 3.91. Found: C, 57.2; H, 9.29; N, 3.80. EI-MS: *m/z* calcd for $[Co(dmamp)(tmhd)]_2$: 716.36 $[M]^+$; found 600 $[\{Co(dmamp)(tmhd)\}_2\text{-}\{dmamp\}]^+$, 425 $[Co(tmhd)_2]^+$, 242 $[Co(tmhd)]^+$.

*[Co(dmamb)(tmhd)]$_2$ (**7**).* $[Co(dmamb)(btsa)]_2$ (**2**) (0.70 g, 1 mmol) and tmhdH (0.32 g, 2 mmol) were used. The crude product was purified by sublimation (130 °C/0.5 Torr) to obtain a pure solid green product. Yield: 0.90 g (63 %), mp 113 °C. FT-IR (KBr, cm^{-1}): 2962(s), 1584(s), 1570(s), 1547(w), 1503(s), 1455(w), 1399(m), 1357(m), 1246(w), 1225(m), 1184(m), 1138(s), 1053(w), 1010(s), 959(w), 926(w), 870(s), 841(w), 789(m), 759(w), 739(w), 618(w), 574(w), 476(m), 424(w). Anal. Calcd for $C_{36}H_{70}N_2O_6Co_2$: C, 58.1; H, 9.47; N, 3.76. Found: C, 58.1; H, 9.47; N, 3.81. EI-MS: *m/z* calcd for $[Co(dmamb)(tmhd)]_2$: 744.39 $[M]^+$; found 614 $[\{Co-$

DOI: 10.1021/acsomega.7b00800
ACS Omega 2017, 2, 5486−5493

(dmamb)(tmhd)}$_2$-{dmamb}]$^+$, 425 [Co(tmhd)$_2$]$^+$, 242 [Co-(tmhd)]$^+$.

Crystallography. Single crystals of **1** were grown from a toluene solution at −30 °C, and single crystals of **3**−**7** were grown from a hexane solution at −30 °C. A specimen of suitable size and quality was coated with paratone oil and mounted onto a glass capillary. Reflection data of **1**, **3**, **4**, **5**, and **6** were collected on a Bruker Apex II-CCD area detector diffractometer, with graphite-monochromated Mo Kα radiation (λ = 0.71073 Å). The hemisphere of reflection data was collected as ω-scan frames with 0.3° per frame and an exposure time of 10 s per frame. Cell parameters were determined and refined using the SMART program.[31] Data reduction was performed using the SAINT software.[32] The data were corrected for Lorentz and polarization effects. An empirical absorption correction was applied using the SADABS program.[33] A crystal of **7** was coated with paratone oil and the diffraction data measured at 173 K with Mo Kα radiation on an X-ray diffraction camera system using an imaging plate equipped with a graphite crystal incident beam monochromator. The RapidAuto software was used for data collection and data processing.[34] The structures were solved by direct methods, and all of the nonhydrogen atoms were subjected to anisotropic refinement by a full-matrix least-squares methods on F2 using the SHELXTL/PC package.[35] Hydrogen atoms were placed at their geometrically calculated positions and were refined based on the corresponding carbon atoms with isotropic thermal parameters. The supplementary crystallographic data for this paper can be found in CCDC 1535120 (complex **1**), 1535122−1535125 (complex **3**−**6**), and 1552487 (complex **7**).

AUTHOR INFORMATION

Corresponding Author

*E-mail: tmchung@krict.re.kr. Phone: +82-42-860-7359.

ORCID

Seung Uk Son: 0000-0002-4779-9302

Myoung Soo Lah: 0000-0001-9517-7519

Taek-Mo Chung: 0000-0002-5169-2671

Notes

The authors declare no competing financial interest.

ACKNOWLEDGMENTS

This research was supported by a Grant from the Development of Organometallics and Device Fabrication for IT/ET Convergence Project through the Korea Research Institute of Chemical Technology (KRICT) of Republic of Korea (SI1703-02). We would like to thank the Center for Chemical Analysis at the Korea Research Institute of Chemical Technology (KRICT) for using their facilities for solving the molecular structures.

REFERENCES

(1) (a) Pollard, M. J.; Weinstock, B. A.; Bitterwolf, T. E.; Griffiths, P. R.; Newbery, A. P.; Paine, J. B. A mechanistic study of the low-temperature conversion of carbon monoxide to carbon dioxide over a cobalt oxide catalyst. *J. Catal.* **2008**, *254*, 218−225. (b) Yang, Q. J.; Choi, H.; Dionysiou, D. D. Nanocrystalline cobalt oxide immobilized on titanium dioxide nanoparticles for the heterogeneous activation of peroxymonosulfate. *Appl. Catal., B* **2007**, *74*, 170−178. (c) Tyczkowski, J.; Kapica, R.; Lojewska, J. Thin cobalt oxide films for catalysis deposited by plasma-enhanced metal-organic chemical vapor deposition. *Thin Solid Films* **2007**, *515*, 6590−6595.

(2) Jeong, Y.-M.; Lee, J.-K.; Ha, S.-C.; Kim, S. H. Fabrication of cobalt-organic composite thin film via plasma-enhanced chemical vapor deposition for antibacterial applications. *Thin Solid Films* **2009**, *517*, 2855−2858.

(3) Nakamura, Y. The Long Journey in Perpendicular Magnetic Recording From the Beginning to the Future Soft Magnetic Materials and Recording Heads. *ECS Trans.* **2007**, *3*, 29−45.

(4) Chioncel, M. F.; Haycock, P. W. Cobalt Thin Films Deposited by Photoassisted MOCVD Exhibiting Inverted Magnetic Hysteresis. *Chem. Vap. Deposition* **2006**, *12*, 670−678.

(5) (a) Jung, H. K.; Lee, H. B.; Tsukasa, M.; Jung, E.; Yun, J. H.; Lee, J. M.; Choi, G. H.; Choi, S.; Chung, C. Formation of highly reliable Cu/low-k interconnects by using CVD Co barrier in dual damascene structures. *IEEE Reliab. Phys. Symp.* 2011, *307*. 10.1109/IRPS.2011.5784492. (b) Yang, C. C.; Flaitz, P.; Wang, P. C.; Chen, F.; Edelstein, D. Characterization of Selectively Deposited Cobalt Capping Layers: Selectivity and Electromigration Resistance. *IEEE Electron Device Lett.* **2010**, *31*, 728−730.

(6) Lee, H.-B.-R.; Kim, H. J. Self-formation of dielectric layer containing $CoSi_2$ nanocrystals by plasma-enhanced atomic layer deposition. *J. Cryst. Growth* **2010**, *312*, 2215−2219.

(7) (a) Londergan, A. R.; Nuesca, G.; Goldberg, C.; Peterson, G.; Kaloyeros, A. E.; Arkles, B.; Sullivan, J. J. Interlayer Mediated Epitaxy of Cobalt Silicide on Silicon (100) from Low Temperature Chemical Vapor Deposition of Cobalt Formation Mechanisms and Associated Properties. *J. Electrochem. Soc.* **2001**, *148*, C21−C27. (b) Kutschera, M.; Groth, T.; Kentsch, C.; Shumay, I. L.; Weinelt, M.; Fauster, Th Electronic structure of $CoSi_2$ films on Si(111) studied using time-resolved two-photon photoemission. *J. Phys.: Condens. Matter* **2009**, *21*, 134006.

(8) (a) Wu, H. B.; Chen, J. S.; Hng, H. H.; Lou, X. W. Nanostructured metal oxide-based materials as advanced anodes for lithium-ion batteries. *Nanoscale* **2012**, *4*, 2526−2542. (b) Woo, J. H.; Trevey, J. E.; Cavanagh, A. S.; Choi, Y. S.; Kim, S. C.; George, S. M.; Oh, K. H.; Lee, S.-H. Nanoscale Interface Modification of $LiCoO_2$ by Al_2O_3 Atomic Layer Deposition for Solid-State Li Batteries. *J. Electrochem. Soc.* **2012**, *159*, A1120−A1124. (c) Scott, I. D.; Jung, Y. S.; Cavanagh, A. S.; Yan, Y.; Dillon, A. C.; George, S. M.; Lee, S.-H. Ultrathin Coatings on Nano-$LiCoO_2$ for Li-Ion Vehicular Applications. *Nano Lett.* **2011**, *11*, 414−418. (d) Jung, Y. S.; Cavanagh, A. S.; Gedvilas, L.; Widjonarko, N. E.; Scott, I. D.; Lee, S.-H.; Kim, G.-H.; George, S. M.; Dillon, A. C. Improved Functionality of Lithium-Ion Batteries Enabled by Atomic Layer Deposition on the Porous Microstructure of Polymer Separators and Coating Electrodes. *Adv. Energy Mater.* **2012**, *2*, 1022−1027. (e) Donders, M. E.; Arnoldbik, W. M.; Knoops, H. C. M.; Kessels, W. M. M.; Notten, P. H. L. Atomic Layer Deposition of $LiCoO_2$ Thin-Film Electrodes for All-Solid-State Li-Ion Micro-Batteries. *J. Electrochem. Soc.* **2013**, *160*, A3066−A3071.

(9) (a) Pratt, W. P. J.; Lee, S.-F; Holody, P.; Yang, Q.; Loloee, R.; Bass, J.; Schroeder, P. A. Giant magnetoresistance with current perpendicular to the multilayer planes. *J. Magn. Magn. Mater.* **1993**, *126*, 406−409. (b) Pratt, W. P.; Lee, S. F.; Yang, Q.; Holody, P.; Loloee, R.; Schroeder, P. A.; Bass, J. Giant magnetoresistance with current perpendicular to the layer planes of Ag/Co and AgSn/Co multilayers (invited). *J. Appl. Phys.* **1993**, *73*, 5326.

(10) (a) Balke, B.; Wurmehl, S.; Fecher, G. H.; Felser, C.; Kübler, J. Rational design of new materials for spintronics: Co_2FeZ (Z = Al, Ga, Si, Ge). *Sci. Technol. Adv. Mater.* **2008**, *9*, 014102. (b) Ernult, F.; Yakushiji, K.; Mitani, S.; Takanashi, K. Spin accumulation in metallic nanoparticles. *J. Phys.: Condens. Matter* **2007**, *19*, No. 165214. (c) Tsymbal, E. Y.; Belashchenko, K. D.; Velev, J. P.; Jaswal, S. S.; van Schilfgaarde, M.; Oleynik, I. I.; Stewart, D. A. Interface effects in spin-dependent tunneling. *Prog. Mater. Sci.* **2007**, *52*, 401−420. (d) Yakushiji, K.; Mitani, S.; Ernult, F.; Takanashi, K.; Fujimori, H. Spin-dependent tunneling and Coulomb blockade in ferromagnetic nanoparticles. *Phys. Rep.* **2007**, *451*, 1−35.

(11) (a) Lee, J.; Park, H. J.; Won, S. H.; Jeong, K. H.; Jung, H. S.; Kim, C.; Bang, H. J.; Lee, C. M.; Kim, J. H.; Kwon, G. C.; Cho, H. L.; Soh, H. S.; Lee, J. G. Consecutive CVD of Al/Co Bilayers on SiO_2 or

DOI: 10.1021/acsomega.7b00800
ACS Omega 2017, 2, 5486−5493

Alq_3 Surfaces at Low Temperature of 70 °C. *J. Electrochem. Soc.* **2007**, *154*, H833−H837. (b) Lee, J. G.; Park, H. J.; Lee, J. G. OTS-Templated Cobalt Deposition Using $Co_2(CO)_8$ Precursor. *Solid State Phenom.* **2007**, *124*−*126*, 531−534. (c) Lee, J.; Yang, H. J.; Lee, J. H.; Kim, J. Y.; Nam, W. J.; Shin, H. J.; Ko; Lee, J. G.; Lee, E. G.; Kim, C. S. Highly Conformal Deposition of Pure Co Films by MOCVD Using $Co_2(CO)_8$ as a Precursor. *J. Electrochem. Soc.* **2006**, *153*, G539−G542. (d) Ye, D. X.; Pimanpang, S.; Jezewski, C.; Tang, F.; Senkevich, J. J.; Wang, G. C.; Lu, T. M. Low temperature chemical vapor deposition of Co thin films from $Co_2(CO)_8$. *Thin Solid Films* **2005**, *485*, 95−100.

(12) (a) Premkumar, P. A.; Turchanin, A.; Bahlawane, N. Effect of Solvent on the Growth of Co and Co_2C Using Pulsed-Spray Evaporation Chemical Vapor Deposition. *Chem. Mater.* **2007**, *19*, 6206−6211. (b) Premkumar, P. A.; Bahlawane, N.; Reiss, G.; Kohse-Hoeinghaus, K. CVD of Metals Using Alcohols and Metal Acetylacetonates, Part II: Role of Solvent and Characterization of Metal Films Made by Pulsed Spray Evaporation CVD. *Chem. Vap. Deposition* **2007**, *13*, 227−231.

(13) (a) Lim, B. S.; Rahtu, A.; Park, J.-S.; Gordon, R. G. Synthesis and Characterization of Volatile, Thermally Stable, Reactive Transition Metal Amidinates. *Inorg. Chem.* **2003**, *42*, 7951−7958. (b) Lim, B. S.; Rahtu, A.; Gordon, R. G. Atomic layer deposition of transition metals. *Nat. Mater.* **2003**, *2*, 749−754. (c) Li, Z.; Gordon, R. G.; Farmer, D. B.; Lin, Y.; Vlassak, J. Nucleation and Adhesion of ALD Copper on Cobalt Adhesion Layers and Tungsten Nitride Diffusion Barriers. *Electrochem. Solid-State Lett.* **2005**, *8*, G182−G185.

(14) (a) Lee, H.-B.-R.; Son, J. Y.; Kim, H. Nitride mediated epitaxy of CoSi2CoSi2 through self-interlayer-formation of plasma-enhanced atomic layer deposition Co. *Appl. Phys. Lett.* **2007**, *90*, No. 213509. (b) Lee, H.-B.-R.; Kim, H. High-Quality Cobalt Thin Films by Plasma-Enhanced Atomic Layer Deposition. *Electrochem. Solid-State Lett.* **2006**, *9*, G323−G325.

(15) Lee, K.; Kim, K.; Park, T.; Jeon, H.; Lee, Y.; Kim, J.; Yeom, S. Characteristics of Ti-Capped Co Films Deposited by a Remote Plasma ALD Method Using Cyclopentadienylcobalt Dicarbonyl. *J. Electrochem. Soc.* **2007**, *154*, H899−H903.

(16) (a) Crawford, N. R. M.; Knutsen, J. S.; Yang, K.-A.; Haugstad, G.; McKernan, S.; McCormick, F. B.; Gladfelter, W. L. Splitting the Coordinated Nitric Oxide in $Co(CO)_3(NO)$ Leads to a Nanocrystalline, Conductive Oxonitride of Cobalt. *Chem. Vap. Deposition* **1998**, *4*, 181−183. (b) Lane, P. A.; Oliver, P. E.; Wright, P. J.; Reeves, C. L.; Pitt, A. D.; Cockayne, B. Metal Organic CVD of Cobalt Thin Films Using Cobalt Tricarbonyl Nitrosyl. *Chem. Vap. Deposition* **1998**, *4*, 183−186. (c) Ivanova, A. R.; Nuesca, G.; Chen, X.; Goldberg, C.; Kaloyeros, A. E.; Arkles, B.; Sullivan, J. J. The Effects of Processing Parameters in the Chemical Vapor Deposition of Cobalt from Cobalt Tricarbonyl Nitrosyl. *J. Electrochem. Soc.* **1999**, *146*, 2139−2145. (d) Deo, N.; Bain, M. F.; Montgomery, J. H.; Gamble, H. S. Study of magnetic properties of thin cobalt films deposited by chemical vapour deposition. *J. Mater. Sci.: Mater. Electron.* **2005**, *16*, 387−892.

(17) Choi, H.; Park, S. Liquid Cobalt (I) Hydride Complexes as Precursors for Chemical Vapor Deposition. *Chem. Mater.* **2003**, *15*, 3121−3124.

(18) Li, Z.; Lee, D. K.; Coulter, M.; Rodriguez, L. N. J.; Gordon, R. G. Synthesis and characterization of volatile liquid cobalt amidinates. *Dalton Trans.* **2008**, *0*, 2592−2597.

(19) Knisley, T. J.; Saly, M. J.; Heeg, M. J.; Roberts, J. L.; Winter, C. H. Volatility and High Thermal Stability in Mid- to Late-First-Row Transition-Metal Diazadienyl Complexes. *Organometallics* **2011**, *30*, 5010−5017.

(20) Pugh, T.; Cosham, S. D.; Hamilton, J. A.; Kingsley, A. J.; Johnson, A. L. Cobalt(III) Diazabutadiene Precursors for Metal Deposition: Nanoparticle and Thin Film Growth. *Inorg. Chem.* **2013**, *52*, 13719−13729.

(21) (a) Lee, W.; Jeon, W.; An, C. H.; Chung, M. J.; Kim, H. J.; Eom, T.; George, S. M.; Park, B. K.; Han, J. H.; Kim, C. G.; Chung, T.-M.; Lee, S. W.; Hwang, C. S. Improved Initial Growth Behavior of SrO and $SrTiO_3$ Films Grown by Atomic Layer Deposition Using $\{Sr(demamp)(tmhd)\}_2$ as Sr-Precursor. *Chem. Mater.* **2015**, *27*, 3881−3891. (b) Lee, S. W.; Kwon, O. S.; Han, J. H.; Hwang, C. S. Enhanced electrical properties of $SrTiO_3$ thin films grown by atomic layer deposition at high temperature for dynamic random access memory applications. *Appl. Phys. Lett.* **2008**, *92*, 222903. (c) Blanquart, T.; Niinistö, J.; Gavagnin, M.; Longo, V.; Pallem, V. R.; Dussarrat, C.; Ritala, M.; Leskelä, M. Novel Heteroleptic Precursors for Atomic Layer Deposition of TiO_2. *Chem. Mater.* **2012**, *24*, 3420−3424. (d) George, S. M.; Park, B. K.; Kim, C. G.; Chung, T.-M. Heteroleptic Group 2 Metal Precursors for Metal Oxide Thin Films. *Eur. J. Inorg. Chem.* **2014**, *2014*, 2002−2010. (e) Kim, H.-S.; George, S. M.; Park, B. K.; Son, S. U.; Kim, C. G.; Chung, T.-M. New heteroleptic magnesium complexes for MgO thin film application. *Dalton Trans.* **2015**, *44*, 2103−2109.

(22) Carl, E.; Demeshko, S.; Meyer, F.; Stalke, D. Triimidosulfonates as Acute Bite-Angle Chelates: Slow Relaxation of the Magnetization in Zero Field and Hysteresis Loop of a CoII Complex. *Chem. − Eur. J.* **2015**, *21*, 10109−10115.

(23) Pasko, S.; Hubert-Pfalzgraf, L. G.; Abrutis, A.; Vaissermann, J. Synthesis and molecular structures of cobalt(II) β-diketonate complexes as new MOCVD precursors for cobalt oxide films. *Polyhedron* **2004**, *23*, 735−741.

(24) Kumar, K. S. S.; Gnanou, Y.; Champouret, Y.; Daran, J.-C; Poli, R. Radical Polymerization of Vinyl Acetate with Bis-(tetramethylheptadionato)cobalt(II): Coexistence of Three Different Mechanisms. *Chem. − Eur. J.* **2009**, *15*, 4874−4885.

(25) Ahmed, M. A. K.; Fjellvåg, H.; Kjekshus, A.; Dietzel, P. D. C. Syntheses, Structures, and Polymorphism of β-Diketonato Complexes − $Co(thd)_3$. *Z. Anorg. Allg. Chem.* **2008**, *634*, 247−254.

(26) Kalutarage, L. C.; Martin, P. D.; Heeg, M. J.; Winter, C. H. Synthesis, Structure, and Solution Reduction Reactions of Volatile and Thermally Stable Mid to Late First Row Transition Metal Complexes Containing Hydrazonate Ligands. *Inorg. Chem.* **2013**, *52*, 5385−5394.

(27) (a) Nandurkar, N. S.; Patil, D. S.; Bhanage, B. M. Ultrasound assisted synthesis of metal-1,3-diketonates. *Inorg. Chem. Commun.* **2008**, *11*, 733−736. (b) Jiang, Y.; Liu, M.; Wang, Y.; Song, H.; Gao, J.; Meng, G. Decomposition Behavior of $M(DPM)_n$ (DPM = 2,2,6,6-Tetramethyl-3,5-heptanedionato; n = 2, 3, 4). *J. Phys. Chem. A* **2006**, *110*, 13479−13486.

(28) Bürger, H.; Wannagat, U. Silylamido-Derivate von Eisen und Kobalt. *Monatsh. Chem.* **1963**, *94*, 1007−1012.

(29) Bradley, D. C.; Fisher, K. J. Bis(hexamethyldisilylamino)cobalt-(II), a two-coordinated cobalt compound. *J. Am. Chem. Soc.* **1971**, *93*, 2058−2059.

(30) (a) Anwander, R.; Munck, F. C.; Priermeier, T.; Scherer, W.; Runte, O.; Herrmann, W. A. Volatile Donor-Functionalized Alkoxy Derivatives of Lutetium and Their Structural Characterization. *Inorg. Chem.* **1997**, *36*, 3545−3552. (b) Heydari, A.; Mehrdad, M.; Malekiand, A.; Ahmadi, N. A New and Efficient Epoxide Ring Opening via Poor Nucleophiles: Indole, p-Nitroaniline, Borane and O-Trimethylsilylhydroxylamine in Lithium Perchlorate. *Synthesis* **2004**, *2004*, 1563−1565.

(31) *SMART*, version 5.0, Data collection software; Bruker AXS, Inc.: Madison, WI, 1998.

(32) *SAINT*, version 5.0, Data integration software; Bruker AXS Inc.: Madison, WI, 1998.

(33) Sheldrick, G. M. *SADABS, Program for Absorption Correction with the Bruker SMART System*; Universitat Gottingen: Germany, 1996.

(34) *Rapid Auto Software*, R-Axis series, Cat. No. 9220B101; Rigaku Corporation.

(35) Sheldrick, G. M. *Acta Crystallogr., Sect. C: Struct. Chem.* **2015**, *71*, 3.

DOI: 10.1021/acsomega.7b00800
ACS Omega 2017, 2, 5486−5493